RESEARCH ARTICLE
doi: 10.2306/scienceasia1513-1874.2021.002

ScienceAsia 47 (2021): **19–29**

Characterization and transcriptomic analysis of *Streptococcus thermophilus* strain EU01 promoted by *Eucommia ulmoides* Oliv. extract

Zhi-Ying Nie, Yu-Hong Li, Lin Li, Xin Zhao*

Key Laboratory of Pharmacology of Traditional Chinese Medical Formulae, Ministry of Education, Tianjin University of Traditional Chinese Medicine, Tianjin 301617 China

*Corresponding author, e-mail: xinaw26@tju.edu.cn

Received 3 May 2020
Accepted 20 Oct 2020

ABSTRACT: *Eucommia ulmoides* Oliv. has been extensively studied for its promoting effect on bacterial growth. A bacterial strain, called EU01, was isolated from the aqueous extract of *E. ulmoides* Oliv. leaves (AEEL). The optimal concentration of AEEL for promoting EU01 was 5 mg/ml, and the optimal cultivating time was 24 h. According to biochemical and physiological tests and genomic analysis, EU01 was identified as a *Streptococcus thermophilus* strain with probiotic potential. Strain EU01 showed strong inhibition against *Staphylococcus aureus*, which was also enhanced by 5 mg/ml AEEL. As such, the inhibitory spectrum and antimicrobial activity of strain EU01 with AEEL were investigated via the Oxford cup method. The transcriptome of strain EU01 was sequenced to explore the mode of action of AEEL on this strain. Among differentially expressed genes (DEGs) responding to AEEL, 66 genes were upregulated, and 229 genes were downregulated. DNA repaired and synthesis related functions were further demonstrated as remarkable differences through gene ontology (GO) and functional pathway analysis, especially associated with probiotic potential. This study suggested that traditional Chinese medicine (TCM) *E. ulmoides* promoting bacteria with probiotic potential might be a novel target for the treatment of diseases by regulating the intestinal flora.

KEYWORDS: *Eucommia ulmoides* Oliv., probiotic potential, transcriptome, DNA repaired and synthesis related functions

INTRODUCTION

In either intestinal or oral microflora, beneficial microorganisms and harmful pathogens coexist and restrict one another, forming a complex and stable microecological environment [1]. Probiotics are the dominant bacterial group in the intestinal tract. They regulate the health of the gastrointestinal tract and promote digestion and absorption [2]. Among gut probiotics, *Streptococcus thermophilus* is a Gram-positive probiotic classified as a Lactobacillales bacterium [3]. *S. thermophilus* is recognized as a safe ingredient widely used in the production of some important fermented dairy products [4]. *S. thermophilus*, used as a beneficial bacterium, also has some functional activities such as the production of extracellular polysaccharides, bacteriocins, and vitamins [5]. Although *S. thermophilus* widely exists in foods and in the digestive system, the isolation of *S. thermophilus* from Chinese herbal medicines has been rarely reported.

Eucommia ulmoides Oliv. (Du-zhong in Chinese) is a valuable and nourishing medicinal plant in China, which nourishes the liver and the kidney, strengthens bones, and calms the fetus [6]. Modern pharmacological studies have confirmed that it has antibacterial, anti-inflammatory, and immune-enhancing effects [7]. *E. ulmoides* also promotes the growth of intestinal probiotics, especially *Bifidobacteria* and *Lactobacillales*, and regulates intestinal microflora disorder [8]. According to the National Health Commission of China, *E. ulmoides* leaves have been added to the new list of traditional Chinese medicine (TCM) that can be used as food and medicine. The interaction between *E. ulmoides* and probiotics along with the isolation of the potential probiotic strain EU01 from *E. ulmoides* is worth studying.

Transcriptomics is a powerful approach to explore changes especially in the gene expression profiling upon host-bacteria interactions whereby several transcriptome-based tools could be utilized [9]. The transcriptomics of TCM plant-microbe interactions have been targets of interest to investigate medicine-microbe interactions [10]. TCM has the characteristics of multiple components and multiple

targets [11]. Single-gene, molecular, and signal pathway analyses are often difficult to be performed to accurately grasp the molecular mechanism of TCM efficacy. However, transcriptional methods can reveal the changes in the whole gene expression in a whole cell. Therefore, this method has been favored by researchers and widely used to explore the efficacy of TCM at genetic level.

High-concentration of *E. ulmoides* has a broad-spectrum bacteriostatic effect that may threaten the microecological balance [12]. Therefore, the effect of proper *E. ulmoides* concentration on the growth of probiotics investigated in this experiment is important. The growth-promoting effects of TCM materials on probiotics are also rarely reported. In this study, we aimed to characterize and identify probiotic strain from the aqueous extract of *E. ulmoides* Oliv. leaves (AEEL) with antimicrobial activity against *Staphylococcus aureus*. In order to explain the effect of AEEL on this strain, growth and antimicrobial activity of strain EU01 were investigated *in vitro*. The transcriptome of this strain was sequenced and analyzed to explore the mechanism of AEEL on it. Genes and pathways associated with growth, probiotic potential and antimicrobial activity affected by AEEL were also predicted. We tried to provide a basis for using AEEL to increase the colonization quantity of probiotics, further promote intestinal and oral health, and expand the coproduction of TCMs and probiotics *in vitro*.

MATERIALS AND METHODS

Medicinal materials and preparation

E. ulmoides Oliv. leaves were collected in August 2017 from the medicinal botanical garden of Jiangxi Pu Zheng Pharmaceutical Co., Ltd. (Jiangxi, China). The leaves of *E. ulmoides* were cut in lab and then extracted with distilled water (volume ratio, 1:8) twice by modified reflux extraction method [13], 1.5 h each time, and AEEL liquor sample was obtained. The liquor sample was then distilled by rotary evaporation at 60 °C with speed of 400 ml/h. Dry extract was collected at 60 °C under vacuum condition for 48 h, and the yield of the extract was calculated to be 33.3%. The extract sample was stored at 4 °C.

Bacteria and cultures

Strains used in this study were preserved at Microbiology Lab of Tianjin University of Traditional Chinese Medicine. Strain EU01 is deposited in the China Pharmaceutical Culture Collection (CPCC) under accession number CPCC 101246. Strain EU01 was activated by transferring single colonies of the strain from plates to 10 ml activation MRS medium extract in 50-ml static flask at 37 °C for 24 h. *S. aureus* ATCC6358, *Escherichia coli* CMCC44103, *Lactococcus lactis* NZ9000, *Bacillus cereus* EP27, *Enterococcus faecalis* EP12, and *Shigella* sp. EP19 were used as the indicator strains in bacteriostatic assay and antimicrobial spectrum detection, which were activated by transferring single colonies of the strain from plates to 3 ml activation LB or MRS medium (Solarbio, Beijing, China) extract in 10-ml flask at 37 °C for 16 h. The screening procedure of strain EU01 and promotion effect of AEEL on strain EU01 were presented in supplementary data S1.

Probiotic potential characterization and identification of EU01

Probiotic potential tests included sugar fermentation, acidic tolerance, bile salt tolerance experiments, and optimum growth temperature measurement and conducted according to Peng and Si [14]. MRS media with 0.5% glucose, sucrose, and maltose were used for sugar fermentation test, and MRS media with pH values of 3.0, 4.0, 5.0, and 7.0 prepared with 37% hydrochloric acid (based on the measured values after autoclave) were used for acidic tolerance test. 0.5%, 1%, and 2% of bile salt was added into MRS medium for bile salt tolerance test, and the medium without bile salt was used as control. Sugar fermentation test was judged by observing discoloration of medium, and acidic tolerance and bile salt tolerance tests were evaluated by plating and colony counting after 3 h of cultivation.

The microorganism EU01 plated on MRS agar medium was picked for Gram staining and observed by microscope according to Microbiology Laboratory booklet. The genomic DNA of strain EU01 was isolated by CTAB method and sequenced using Pacific Biosciences RS sequencing technology (Pacific Biosciences, Menlo Park, CA) by Novogene Co., Ltd. (Beijing, China). According to sequencing results, the closest relative was searched in GenBank database using NCBI-nBLAST. Combined with GenBank in the genus *Streptococcus* sequences using MEGA 6.0 software by the neighbor-joining analysis [15], phylogenetic tree was constructed.

Bacteriostatic activity of strain EU01

The spectrum of antimicrobial activity of strain EU01 was determined by screening against cultures

of *S. aureus* ATCC6358, *E. coli* CMCC44103, *L. lactis* NZ9000, *B. cereus* EP27, *E. faecalis* EP12, and *Shigella* sp. EP19 using the Oxford cup method [16]. *S. aureus* was used as the indicator strain for the following assay to detect the effect of AEEL on the antimicrobial activity of the strain. Equal volume of sterilized Milli-Q water and 0.4 mg/ml gentamicin was used as negative control and positive control, respectively. Plates were cultivated at 37 °C for 24 h, and antimicrobial circle diameter was measured. Each experiment was repeated 3 times.

Statistical analysis

All statistical analysis was completed by Microsoft Office EXCEL 2007 and SPSS software. Measurement data were expressed by mean ± standard deviation, and one-way ANOVA was used for statistical analysis. The homogeneity of variance was tested. If the data variance was homogeneous, LSD test would be used; if the data variance was not uniform, Dunnett-t3 test would be used. The difference was statistically significant with $*/^{\#}$ $p < 0.05$ or $**/^{\#\#}$ $p < 0.01$.

RNA Extraction and sequencing

The total RNA of strain EU01 co-cultured with 5 mg/ml AEEL and strain EU01 was isolated with the RNAprep pure Cell/Bacteria Kit (TIANGEN DP430, China) according to the manufacturer's guidelines [17]. Agarose gel electrophoresis was used to analyze the degree of RNA degradation and whether there was any contamination. The purity of RNA was detected by NanoPhotometer (IMPLEN, USA). Ribo-Zero™ rRNA Removal Kit (Illumina, USA) was used to remove rRNA from qualified samples to enrich mRNA. Fragmentation buffer was added to break mRNA into short fragments. Single-stranded cDNA was synthesized by using mRNA as a template with 6 base random primers (random hexamers). And then, double-stranded cDNA was synthesized by adding buffer solution, dNTPs (dUTP instead of dNTP), DNA polymerase I, and RNase H. In order to select cDNA fragments of preferentially 150–200 bp in length, the library fragments were purified with AMPure XP system (Beckman Coulter, USA). Then, 3 μl USER Enzyme (NEB, USA) was used with size-selected, adaptor-ligated cDNA at 37 °C for 15 min followed by 5 min at 95 °C before PCR. Then, PCR was performed with Phusion High-Fidelity DNA polymerase, Universal PCR primers, and Index (X) Primer. At last, products were purified (AMPure XP system), and library quality was assessed on the Agilent Bioanalyzer 2100 system. RNA sequencing was conducted at Illumina HiSeq 2500 (Illumina, USA) in Novogene, Beijing, China.

Transcriptomic analysis

The raw RNA-Seq reads were obtained and qualified during base calling by Illumina Casava 1.8; the error rate of each base sequencing was transformed by sequencing Phred value through the formula (Qphred $= -10\log_{10} e$). Afterwards, the raw sequence was filtered in order to remove the adapter sequence and low-quality sequence. And then, clean reads were mapped against the reference genome sequence of each strain. Genomic localization analysis of filtered sequencing sequences was conducted by Bowtie2-2.2.3 [18]. The level of gene expression was judged by counting the sequence (reads) located in the genomic region or gene coding region and analyzed by HTSeq software v0.6.1, and the model used was Union [19]. Moreover, expected number of Fragments Per Kilobase of transcript sequence per Million base pairs sequenced (FPKM) was generated. The read count was normalized and modelized for gene differential expression analysis by DEGseq [20]. The significance threshold was q-value < 0.005 and $|\log_2(\text{fold change})| > 1$ ($\log_2$(sample1/sample2)). Gene Ontology (GO) enrichment analysis of differentially expressed genes (DEGs) was implemented by the GOseq R package, in which gene length bias was corrected [21]. GO terms with corrected p-value less than 0.05 were considered significantly enriched by differential expressed genes. Functional pathway enrichment analyzation was performed by Kyoto Encyclopedia of Genes and Genomes (KEGG) on KOBAS (2.0), including metabolic analysis and metabolic network research in organisms [22].

RESULTS

Isolation and probiotic potential characterization of strain EU01

By applying an overlaid indicator strain method, an isolate named EU01 from AEEL showed a distinct inhibition against *S. aureus*. With isolation of EU01, colony of this isolate was cultured for probiotic potential investigation. The colony of strain EU01 on MRS agar plate was white and round with smooth surface, even edges, and stickiness and displayed as Gram-positive coccoid bacteria under microscopy. Based on the biochemical character of probiotic, glucose, sucrose, and maltose were used for sugar fermentation test. After 48 h of incubation at 37 °C, it was observed that the medium color changed from

Table 1 Probiotic potential test result of strain EU01.

Strain	Sugar			Survival rate with different pH				Survival rate with different concentration of bile salt			
	glucose	sucrose	maltose	3.0	4.0	5.0	7.0	0	0.5%	1.0%	2.0%
EU01	+	+	−	65.3%	95.2%	99.4%	100%	100%	99.3%	99.3%	99.2%

+ indicates positive-reaction, − indicates negative-reaction.

purple to yellow in glucose and sucrose fermentation tubes, but the maltose fermentation medium did not change, which indicated that strain EU01 could ferment glucose and sucrose. Considering that survival rate of strain EU01 under the condition of pH 7.0 and without bile salt was 100% (control), survival rate under other conditions was calculated as colony numbers divided by control (Table 1). Under pH 3.0, the number of EU01 decreased to 65% after 3 h of cultivation while the survival rate was 95% under pH 4. After growing with 0.5%, 1%, and 2% bile salts for 3 h, the number of EU01 did not decrease compared with the number without bile salts. The optimum culture condition was at 37–40 °C.

Identification of strain EU01 by genomic-sequencing

Genomic DNA prepared from strain EU01 was sequenced using Pacific Biosciences RS sequencing technology (Pacific Biosciences, Menlo Park, CA), yielding 100 average genome coverage. The sample was prepared as a 10-kb insert library by SMRT bell TM Template kit (version 1.0) and sequenced on PacBio Sequel Systems. The SMRT Link v5.0.1 workflow (PacBio DevNet; Pacific Biosciences) was used to perform a *de novo* assembly. The complete genome sequence of EU01 was composed of a circular contig of a 1948689-bp chromosome with a G+C value of 38.94%. By blasting in GenBank, sequence showed high similarity (minimum identity 99.79%) with *S. thermophilus* strain JIM 8232 and *S. thermophilus* strain TSGB1184. The phylogenetic tree (Fig. 1) showed that the most probable identity might belong to *S. thermophilus*. Combined with physiological and biochemical results, it was identified as *S. thermophilus* EU01 with probiotic potential. The genome was larger than that of strains JIM 8232, KLDS 3.1003, and ST3 but smaller than that of strain NCTC12958. The chromosome consisted of 2165 genes, 3 sRNAs, 18 rRNAs (5S, 16S, and 23S), and 67 tRNAs. Remarkably, based on BAGEL4 and antiSMASH mining, 5 AOI's (Areas of interest) including 1 Streptide, 1 BlpD, 2 Sactipeptides, and 1 NRPS-like peptide were detected in EU01, contributing its antimicrobial activity against *S. aureus* (Table S1). The genome sequence of *Streptococcus thermophilus* EU01 has been deposited in Genbank under the accession number CP047191.1.

Effect of AEEL on the bacteriostatic activity of strain EU01

Antimicrobial spectra of strain EU01 were determined based on the degree of growth inhibition of some microbes by direct antagonism on agar plates using Oxford cup method. In this study, strain EU01 showed inhibition against *S. aureus* ATCC6358 (inhibition zone > 10 mm), *B. cereus* EP27 (inhibition zone > 10 mm), *L. lactis* NZ9000 (5 mm < inhibition zone < 10 mm), and *E. faecalis* EP12 (5 mm < inhibition zone < 10 mm), but it had weak inhibition on *E. coli* CMCC44103 (1 mm < inhibition zone < 5 mm) and *Shigella* sp. EP19 (1 mm < inhibition zone < 5 mm). Antibiotic control by gentamicin showed strong inhibition against all the indicator strains with inhibition zone >15 mm. The bacteriostatic effect of strain EU01 with 5 mg/ml AEEL on *S. aureus* was stronger than that without 5 mg/ml AEEL (Fig. 2a). Previous results indicated that 5 mg/ml AEEL had no bacteriostatic effect on *S. aureus*. We doubted whether the increase of bacterial quantity leads to the increase of bacteriostatic activity. Therefore, 4.8×10^6 CFU/ml strain EU01 were inoculated without AEEL, and the final biomass after 24 h of 4.0×10^7 CFU/ml was used for testing, whose biomass was the same as 2.4×10^6 CFU/ml inoculum culture co-cultured with 5 mg/ml AEEL for 24 h. The supernatant of 4.0×10^7 CFU/ml strain EU01 with 5 mg/ml AEEL was also used for activity testing. In Fig. 2b, antibacterial results indicated that the activities of 4.0×10^7 CFU/ml strain with 5 mg/ml AEEL and its supernatant were stronger than those of 4.0×10^7 CFU/ml strain and its supernatant; the activities of 4.0×10^7 CFU/ml strain and its supernatant were stronger than that of 3.2×10^7 CFU/ml strain EU01. This demonstrated that 5 mg/ml AEEL could not only play an important role in promoting the

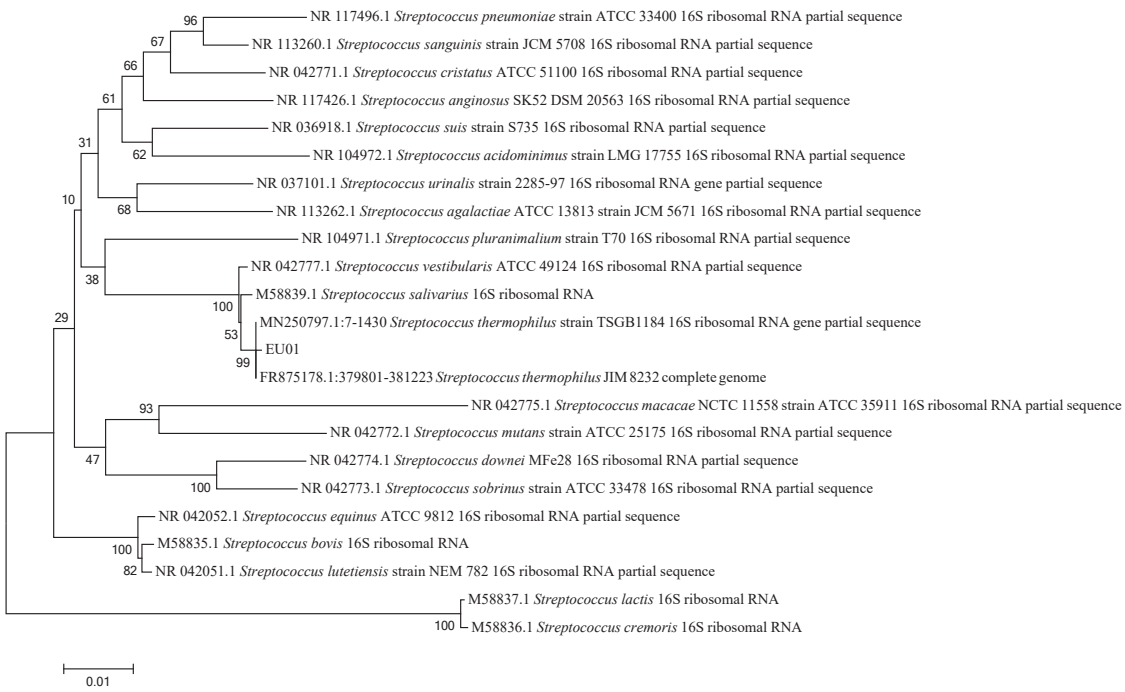

Fig. 1 Phylogenetic tree based on the 16S rDNA sequences showing the position of strain EU01. The type strains of *Streptococcus* sp. and representatives of some other related taxa. Scale bar represents 0.01 substitutions per nucleotide position.

Table 2 A comparison of the sequencing data of *Streptococcus* sp. strains with/without AEEL.

Sample	Raw read	Clean read	Error (%)	GC (%)
strain EU01	12594630	12393176	0.03	42.52
strain EU01+AEEL	13117678	12832104	0.03	42.53

growth of strain EU01, but also in promoting its antimicrobial activity.

Global transcriptional profiles of strain EU01 in response to AEEL

About 12–13 million reads were generated by RNA-Seq for each sample, of which 92–93% passed the quality filtering (Phred quality scores of > 30) using the Illumina Casava version 1.8 (Table 2). Subsequently, the filtered reads were mapped on the genome of EU01 to deduce the FPKM value of each gene or RNA. The FPKM values were used to compare the transcriptomes of the strains and expression level using the HTSeq and shown in violin map (Fig. 3a). The width of each violin represents the number of genes under that expression level. Gene expression level of strain EU01 co-cultured with AEEL was higher than that without AEEL. DEGs were shown in the volcano graph (Fig. 3b). Results indicated the overall distribution of DEGs and the number of DEGs in each comparison group and the overlap relationship between the comparison groups. In the strain EU01, genes were significantly changed by AEEL. Of those, 66 genes were upregulated, and 229 genes were downregulated (Fig. 3b). The detail information of DEGs was presented in supplementary Tables S2 and S3.

DEGs showed opposite trends between normal culture and AEEL

In this study, the relative expression level of different genes was clustered for analysis to determine the expression of different genes under different experimental conditions. The isolated strain EU01 responded to AEEL with an upregulated of 66 genes, and 12 of them were significantly upregulated, whereas 19 of 229 downregulated genes were significantly downregulated which were close to higher cutoff values (q-value < 0.005 and $|\log_2(\text{fold change})| > 1$) (Fig. 4, Tables S2 and S3). Among the altered

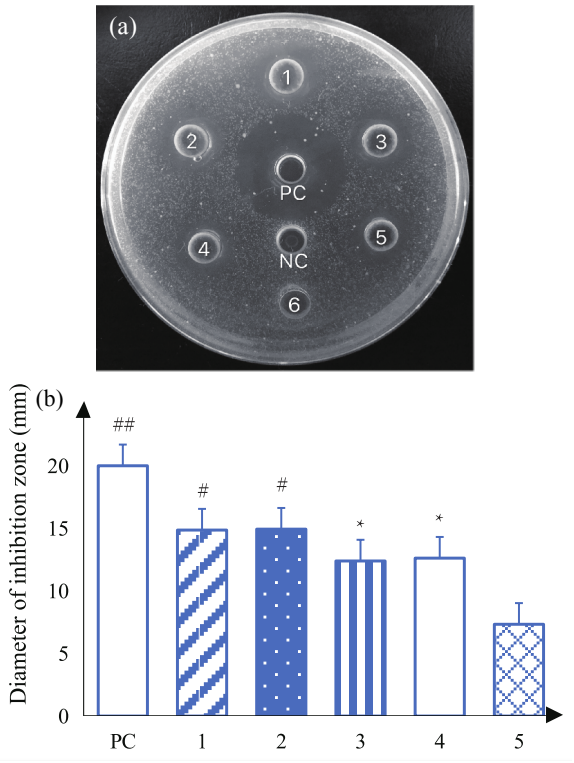

Fig. 2 Antimicrobial activity of strain EU01 with AEEL against *S. aureus*. (a) Bacteriostatic activity measurement by Oxford cup method. Each 30 µl of tested culture was added into each hole including: 1, 4.0×10^7 CFU/ml strain EU01 with 5 mg/ml AEEL; 2, supernatant of 4.0×10^7 CFU/ml strain EU01 with 5 mg/ml AEEL; 3, 4.0×10^7 CFU/ml strain EU01; 4, supernatant of 4.0×10^7 CFU/ml strain EU01; 5, 3.2×10^7 CFU/ml strain EU01; 6, 5 mg/ml AEEL; NC, negative control Milli-Q water; PC, 0.4 mg/ml gentamicin. (b) Diameter measurement of inhibition zone ($^{\#}p<0.05$, $^{\#\#}p<0.01$ versus sample 3, and $^{*}p<0.05$ versus sample 5; data are represented as mean ± SD).

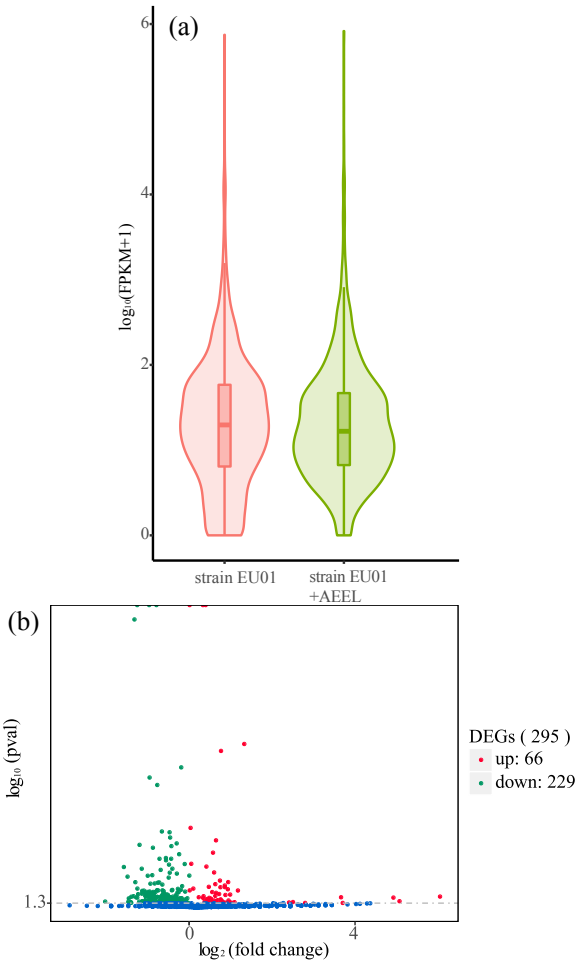

Fig. 3 Comparison of gene expression levels and screening of DEGs. (a) Violin diagram of FPKM. The width of each violin represents the number of genes under that expression level. (b) Volcano map of DEGs. Significant DEGs ($p<0.05$) were presented by red dots (upregulated) and green dots (downregulated) while non-significant DEGs were presented by blue dots.

DEGs related to growth-promoting, antimicrobial activity, and probiotic potential, glucan-binding protein [23], competence protein CoiA [24], DNA repair protein RecO [25], ammonium transporter [26], CHAP domain-containing protein [27], DNA internalization-related competence protein ComEC/Rec2 [28], membrane protein, ABC transporter permease, cold-shock protein, hypothetical protein, and VanZ family protein [29] were significantly upregulated, whereas several ribosomal proteins, metabolic pathway enzymes, amino acid-tRNA ligase, and peptidases were significantly downregulated.

DEGs of GO enrichment analysis of AEEL on strain EU01

GO accessions are divided into 3 parts for analysis including molecular function, biological process, and cellular component. 1227 GO accessions were represented in the GO terms and hence used to perform ortholog analyses. As shown in Fig. 5, genes in 55 GO accessions were mostly assembled. Among them, a large part of the genes is characterized or predicted to belong to the biological process group and others belong to the molecular function and cellular component groups. The most enriched GO terms were mainly impli-

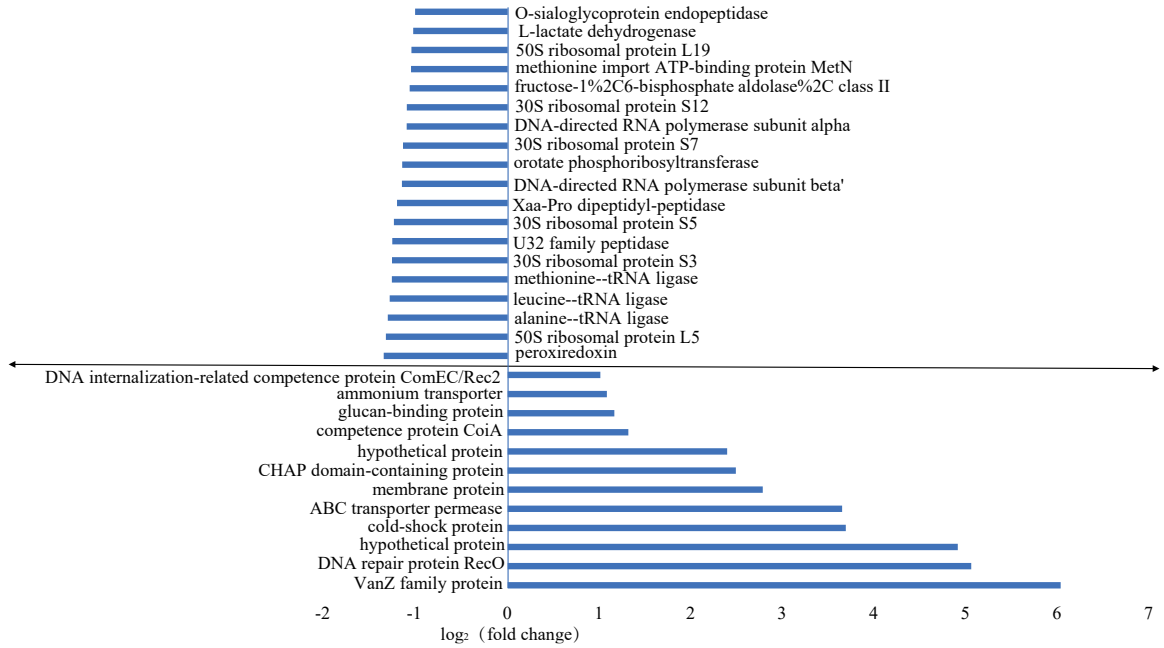

Fig. 4 Analysis of DEGs with cutoff value (q-value < 0.005 and $|\log_2(\text{fold change}| > 1$). The bigger the $|\log_2(\text{fold change}|$ value, the bigger the difference multiples. $\log_2(\text{fold change of upregulated genes} > 0$, $\log_2(\text{fold change of downregulated genes} < 0$.

cated in cellular macromolecule biosynthetic process, macromolecule biosynthetic process, cellular nitrogen compound biosynthetic process, and gene expression. Apart from this, the upregulated genes were mainly implicated in metabolic process, cellular process, primary metabolic process, organic substance metabolic process, catalytic activity, and cellular metabolic process, while many of the significantly downregulated genes were involved in metabolic process, cellular process, organic substance metabolic process, primary metabolic process, catalytic activity, and binding. It was remarkable that DNA repaired and synthesis genes in DEGs were mostly participated in GO terms which suggested that the probiotic potential of strain EU01 altered by AEEL might be associated with DNA [30]. Taken together, the results showed clear differences in gene expression changes between control group without extracts and EU01 in response to AEEL.

DEGs of KEGG enrichment analysis of AEEL on strain EU01

In organisms, different genes coordinate with each other to perform their biological functions. The main biochemical metabolic pathways and signal transduction pathways in which DEGs participated could be determined by pathway significant enrichment. In this study, 2 *Streptococcus* samples were mapped to reference standard pathways to obtain significant enrichment of DEGs. 523 DEGs were matched to multiple KEGG pathways, and 58 AEEL-related KEGG pathways were analyzed by online analysis tool (Table S4). The 5 most representative enrichment pathways were "Metabolic pathways, Biosynthesis of secondary metabolites, Biosynthesis of antibiotics, Ribosome, and Microbial metabolism in diverse environments" with the gene proportion of 16.8%, 7.1%, 6.3%, 5.7%, and 4.6%, respectively. Although the gene proportion was not so high, p-values of "Glycolysis/Gluconeogenesis, RNA degradation, and Oxidative phosphorylation" were less than 0.05. There are a lot of changes in gene expression in these 3 metabolic pathways. Among these pathways, gene encoding enolase, one of the key enzymes in glycolysis, and gene encoding PolC-type DNA polymerase III catalyzing synthesis of new DNA strands were most commonly present in these pathways and upregulated with p-value < 0.005. The annotation information of KEGG enrichment provides valuable resources for the study of AEEL on regulation pathways of *Streptococcus* growth and antimicrobial and probiotic potential factors.

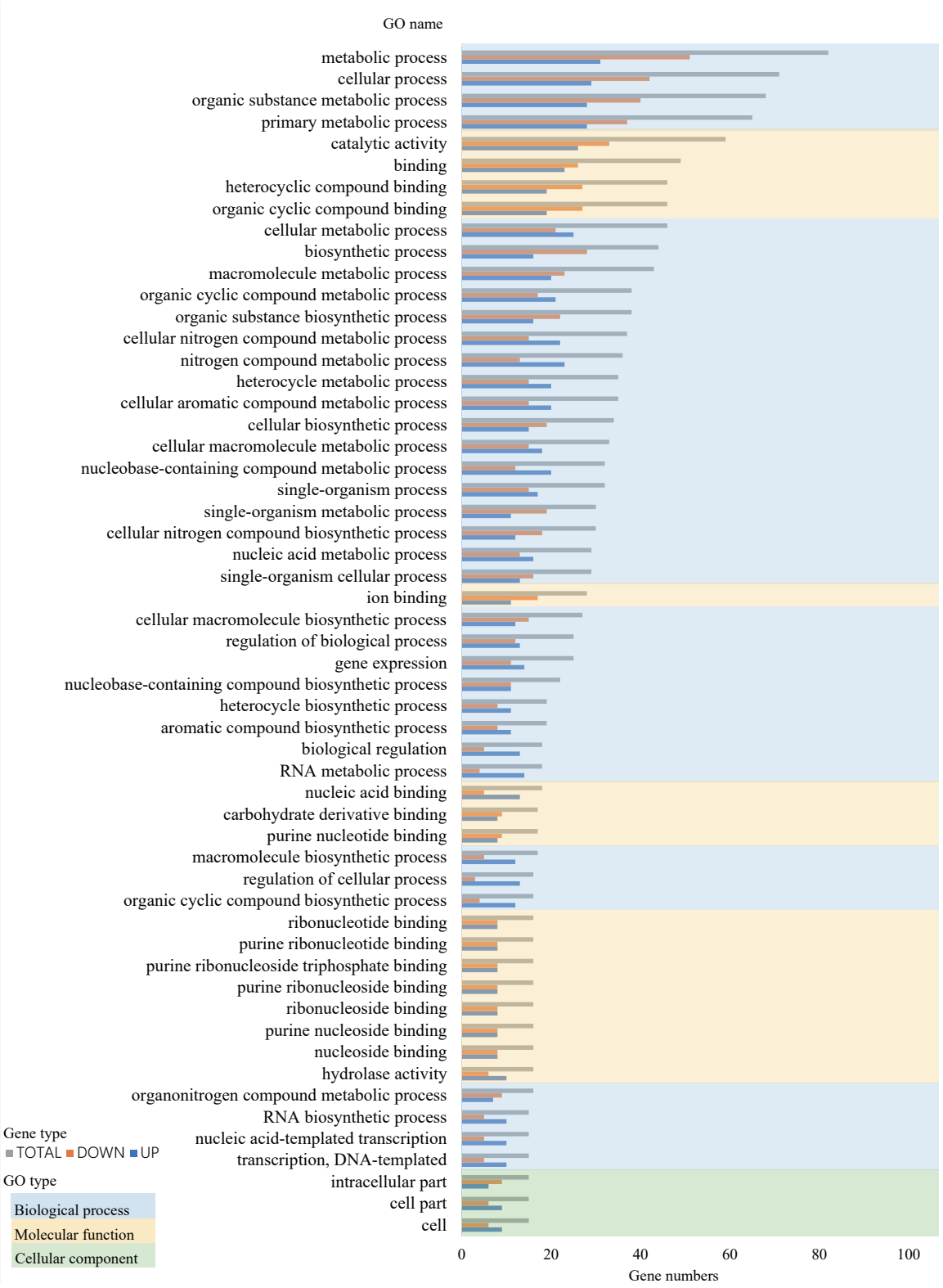

Fig. 5 GO enrichment histogram of DEGs. Different background colors are used to distinguish different GO terms: biological processes, cellular components, and molecular functions and classify up and down of DEGs in each GO term. Upregulated genes are presented in blue, downregulated genes are presented in orange, and total genes are presented in grey.

DISCUSSION

The most probable identity of the isolate strain EU01 might belong to *S. thermophilus*, which is considered "generally recognized as safe (GRAS)" component [4]. Discovering the relationship between *E. ulmoides* and EU01 might be beneficial to intestinal flora and health. Crude drug with low concentration of 5 mg/ml could significantly promote the growth of *Streptococcus* which has never been reported before. The growth of strain EU01 could be inhibited by AEEL at a concentration of 40 mg/ml. It might be because the nutritional components of *E. ulmoides* Oliv. such as polysaccharides, amino acids, vitamins, and trace elements provide growth factors, while the concentration of chlorogenic acid, glycopeptides, and other active substances with bacteriostatic effect increases with higher concentration of AEEL, which produces a dose-effect relationship, and inhibits the growth of EU01 [31]. Moreover, AEEL might provide various effective substances for strain EU01 and promote strain metabolizing and secreting which was beneficial to growth. When the effect of inhibiting pathogenic bacteria was achieved, the effect of inhibiting probiotics also happened, and long-term application *in vivo* might cause human micro-ecological imbalance. Recent studies indicated that *E. ulmoides* Oliv. can promote the growth of *Lactobacillus acidophilus* [32] and reduce the number of *E. coli* and *Salmonella*. AEEL might inhibit the growth of pathogenic bacteria by promoting the growth of probiotics, increase the number of probiotics, reduce the number of pathogenic bacteria, optimize the structure of intestinal flora, and exert a tonic effect.

The transcription levels related to translation, lipid transport and metabolism, and intracellular transport and secretion in lactic acid bacteria have been significantly changed under various conditions, especially in translation-related genes [33]. In this study, we detected the transcription level by GO and KEGG analysis of strain EU01 in the late growth stage with the upregulated genes involved in metabolic process, cellular process, primary metabolic process, organic substance metabolic process, catalytic activity, and cellular metabolic process, while many of the significantly downregulated genes were involved in metabolic process, cellular process, organic substance metabolic process, primary metabolic process, catalytic activity, and binding. Scientists also showed that the characteristics of cell transcriptome changed by time sequence obviously, including that the accumulation and metabolism of energy and substance were dominant in the early growth stage, cell cycle metabolism was dominant in the logarithmic growth stage, and life activity was dominant in the late growth stage to exclude excess metabolites [34].

Genetically, metabolic pathways, biosynthesis of secondary metabolites, biosynthesis of antibiotics, ribosome, and microbial metabolism in diverse environment pathway and DNA repair pathway were significantly affected by AEEL. There might be proteins coded by significantly upregulated DEGs related to bacterial growth, antimicrobial activity, and probiotic potential. Ammonium uptake is facilitated by a family of integral membrane proteins known as ammonium transporters found in all domains of life which might promote the synthesis of proteins or nucleic acids [26]. Glucan-binding proteins, which bind to glucose on bacterial surfaces, contribute to bacterial adhesion [23]. The competence-induced protein, CoiA and ComEC/Rec2, promotes processing of donor DNA after uptake during genetic transformation in *Streptococcus* strains [24, 28]. Sundarrajan et al [27] indicated that bacteriophage-derived CHAP domain protein, P128, could kill *Staphylococcus* cells by cleaving interpeptide cross-bridge of peptidoglycan, which might be related to the bacteriostatic activity of strain EU01. RecO is essential for DNA damage repair in bacteria [25]. There are several antibiotic resistance-related genes putatively coding for a VanZ family protein in the genome of *L. lactis* subsp. *lactis* NCDO 2118 [29].

To elucidate the complex adaptation mechanisms of probiotic potential with AEEL, several genetic and omics studies on stress conditions, production of antimicrobials, and adhesion to the host have been conducted in an attempt to identify gene expression and/or protein production patterns [35]. Genes implicated in DNA repair have been found to be upregulated under acidic stress [30]. Permeases of the major facilitator superfamily and ABC (ATP-binding cassette) transporters have been found to be upregulated, which could play a role in bile expulsion [36]. These reports corresponded to the results of our transcriptome analysis, indicating that AEEL might promote the probiotic potential through altering genes of DNA repair, stress, antimicrobials, and adhesion. Based on probiotic potential tests and genetic analysis of EU01 altered by AEEL, it was further identified as a potential probiotic. In the future, the role of genes in response to *E. ulmoides* can be verified by further molecular genetic experiments.

Some TCMs or compound prescriptions can help maintain the balance of intestinal microecology and

regulate the structure and diversity of gut microbiota (GM) [37]. Metabolites produced by well-growing probiotics, especially antimicrobial substances, indirectly inhibit the growth of pathogenic microorganisms [38]. Through the intervention of *Ganoderma lucidum* water extract, the abundance of the obesity-related bacteria *Enterococcus* and the proportion of *Firmicutes* to *Bacteroides* decreased in mice fed with a high-fat diet [39]. TCM is the most important means in the clinical treatment of diseases and physical fitness. Through the digestive tract, TCM plays an important role in treating local or systemic infection. The digestive tract, especially the intestine, is the main organ where microorganisms parasitize. The bioconversion of TCM by gut microbiota is dominated by hydrolysis and supplemented by oxidation-reduction reactions [40]. Gut microbiota produces substances with pharmacological activities from the metabolism of TCM ingredients and provides a reference for the research on the metabolism of TCM. TCM has less toxic side effects, easy access to materials, and economic benefits, thereby contributing to the development and application of various TCMs. Our study offers a guide for studies on the mechanism of TCMs in the treatment of diseases by regulating the intestinal flora and the development of TCMs as new flora regulators coproduced with probiotics.

CONCLUSION

E. ulmoides possesses a promoting activity for the growth of *S. thermophilus* EU01. The *in vitro* experiments revealed that the AEEL facilitates the growth and antimicrobial activity of EU01 at the concentration of 5 mg/ml. By RNA sequencing and probiotic potential and antimicrobial mechanism analysis, genes encoding DNA repair and synthesis were investigated to be significantly upregulated by AEEL. Our result provides fundamental basis for further studies on *E. ulmoides*-probiotic therapies on diseases and expands the scope in clinical practice.

Appendix A. Supplementary data

Supplementary data associated with this article can be found at http://dx.doi.org/10.2306/scienceasia1513-1874.2021.002.

Acknowledgements: This work was supported by National Natural Science Foundation of China under Grant No. 81803959, Tianjin Municipal Education Commission under Grant No. 2017KJ142, and Tianjin Natural Science Foundation under Grant No. 18JCQNJC83300.

REFERENCES

1. Holzapfel WH, Haberer P, Snel J, Schillinger U, Huis in't Veld JH (1998) Overview of gut flora and probiotics. *Int J Food Microbiol* **41**, 85–101.
2. Pessione E (2012) Lactic acid bacteria contribution to gut microbiota complexity: lights and shadows. *Front Cell Infect Microbiol* **2**, ID 86.
3. Azad M, Sarker M, Li T, Yin J (2018) Probiotic species in the modulation of gut microbiota: an overview. *Biomed Res Int* **2018**, 1–8.
4. Delorme C (2007) Safety assessment of dairy microorganisms: *Streptococcus thermophilus*. *Int J Food Microbiol* **126**, 274–277.
5. Bolotin A, Quinquis B, Renault P, Sorokin A, Ehrlich SD, Kulakauskas S, Lapidus A, Goltsman E, et al (2004) Complete sequence and comparative genome analysis of the dairy bacterium *Streptococcus thermophilus*. *Nat Biotechnol* **22**, 1554–1558.
6. Hussain T, Tan B, Liu G, Oladele OA, Rahu N, Tossou MC, and Yin Y (2016) Health-promoting properties of *Eucommia ulmoides*: a review. *Evid Based Complement Alternat Med* **12**, 1–9.
7. He X, Wang J, Li M, Hao D, Yang Y, Zhang C, He R, Tao R (2014) *Eucommia ulmoides* Oliv.: ethnopharmacology, phytochemistry and pharmacology of an important traditional Chinese medicine. *J Ethnopharmacol* **151**, 78–92.
8. Yang J, Chen H, Peng D, Chen J (2009) Effect of ten kinds of traditional Chinese medicine on the growth of yogurt fermentation bacteria. *Food Sci Technol* **3**, 17–20.
9. Nathan S (2020) Transcriptome profiling to understand host-bacteria interactions: Past, present and future. *ScienceAsia* **46**, 503–512.
10. Li L, Tetu SG, Paulsen IT, Hassan KA (2018) A transcriptomic approach to identify novel drug efflux pumps in bacteria. *Methods Mol Biol* **1700**, 221–235.
11. Li S (2016) Exploring traditional Chinese medicine by a novel therapeutic concept of network target. *Chin J Integr Med* **22**, 647–652.
12. Ji Z, Su Y (2008) Study on antimicrobial activities from *Eucommia ulmoides* Oliv. leaves. *Chem Ind For Prod* **28**, 63–66.
13. Li H, Zhang Z, Li Y, Lei H, Li Z, Zhang Y (2007) Simultaneous determination of several polyphenolic acids in *Eucommia ulmodies* by HPLC: comparison of microwave and ultrasound-assisted extraction with heat reflux extraction techniques for the extraction of polyphenolic acids. *J Jishou Univ (Nat Sci)* **28**.
14. Peng L, Si H (2011) Isolation and identification of *Streptococcus thermophilus* from acidophilus milk. *Mod Agr Sci Tech* **15**, 359–360.
15. Tamura K, Stecher G, Peterson D, Filipski A, Kumar S (2013) MEGA6: Molecular evolutionary genetics analysis version 6.0. *Mol Biol Evol* **30**, 2725–2729.
16. Zhang Y, Zhang QJ, Feng XH, Li S, Xia J, Xu H (2012) A novel agar diffusion assay for qualitative

and quantitative estimation of epsilon-polylysine in fermentation broths and foods. *Food Res Int* **48**, 49–56.
17. Wu D, Huang W, Duan Q, Li F, Cheng H (2014) Sodium houttuyfonate affects production of N-acyl homoserine lactone and quorum sensing-regulated genes expression in Pseudomonas aeruginosa. *Front Microbiol* **5**, ID 635.
18. Langmead B, Salzberg SL (2012) Fast gapped: read alignment with Bowtie 2. *Nat Methods* **9**, 357–359.
19. Anders S, Pyl PT, Huber W (2015) HTSeq-a Python framework to work with high-throughput sequencing data. *Bioinformatics* **31**, 166–169.
20. Anders S, Huber W (2010) Differential expression analysis for sequence count data. *Genome Biol* **11**, ID R106.
21. Young MD, Wakefield MJ, Smyth GK, Oshlack A (2010) Gene ontology analysis for RNA-seq: accounting for selection bias. *Genome Biol* **11**, ID R14.
22. Xie C, Mao X, Huang J, Ding Y, Wu J, Dong S, Kong L, Gao G (2011) KOBAS 2.0: a web server for annotation and identification of enriched pathways and diseases. *Nucleic Acids Res* **39**, W316–W322.
23. Douglas CWI, Russell RRB (1982) Effect of specific antisera on adherence properties of the oral bacterium *Streptococcus mutans*. *Arch Oral Biol* **27**, 1039–1045.
24. Desai BV, Morrison DA (2006) An unstable competence-induced protein, CoiA, promotes processing of donor DNA after uptake during genetic transformation in *Streptococcus pneumoniae*. *J Bacteriol* **188**, 5177–5186.
25. Xu G, Wang L, Chen H, Lu H, Ying N, Tian B, Hua Y (2008) RecO is essential for DNA damage repair in *Deinococcus radiodurans*. *J Bacteriol* **190**, 2624–2628.
26. Li B, Merrick M, Li S, Li H, Zhu S, Shi W, Su Y (2009) Molecular basis and regulation of ammonium transporter in rice. *Rice Sci* **16**, 314–322.
27. Sundarrajan S, Raghupatil J, Vipra A, Narasimhaswamy N, Saravanan S, Appaiah C, Poonacha N, Desai S, et al (2014) Bacteriophage-derived CHAP domain protein, P128, kills *Staphylococcus* cells by cleaving interpeptide cross-bridge of peptidoglycan. *Microbiology* **160**, 2157–2169.
28. Traglia GM, Chua K, Centrón D, Tolmasky ME, Ramírez MS (2014) Whole-genome sequence analysis of the naturally competent *Acinetobacter Baumannii* clinical isolate A118. *Genome Biol Evol* **6**, 2235–2239.
29. Oliveira LC, Saraiva TDL, Silva WM, Pereira UP, Campos BC, Benevides LJ, Rocha FS, Figueiredo HCP, et al (2017) Analyses of the probiotic property and stress resistance-related genes of *Lactococcus lactis* subsp. *lactis* NCDO 2118 through comparative genomics and *in vitro* assays. *PLoS One* **12**, e0175116.
30. Jin J, Zhang B, Guo H, Cui J, Jiang L, Song SH, Sun MB, Ren FZ (2012) Mechanism analysis of acid tolerance response of *Bifidobacterium longum* subsp. *longum* BBMN 68 by gene expression profile using RNA-sequencing. *PLoS One* **7**, e50777.
31. Zhao X, Zhang A, Zhang T, Gao J, Zhang Y (1999) A study on the polysaccharides of *Eucommia ulmoides* leaves. *J Northwest Forestry College* **14**, 73–75.
32. Jia Y, Li M, Chen R, Jiang Y, Ming Z, Zhao P, Pang GC, Yan YL, et al (2016) Effect of *Eucommia ulmoides* Oliv. bark aqueous extract on the growth and fermentation products of *Lactobacillus acidophilus*. *Food Sci* **37**, 147–153.
33. Ravcheev DA, Best AA, Sernova NV, Kazanov MD, Novichkov PS, Rodionov DA (2013) Genomic reconstruction of transcriptional regulatory networks in lactic acid bacteria. *BMC Genomics* **14**, ID 94.
34. Lin X, Wang Z, Li Y, Li J (2016) Genome-wide transcriptional response of the arctic bacterium *Pseudoalteromonas* sp. A2 to oxidative stress induced by hydrogen peroxide. *Acta Oceanol Sin* **35**, 73–80.
35. Papadimitriou K, Zoumpopoulou G, Foligné B, Alexandraki V, Kazou M, Pot B, Tsakalidou E (2015) Discovering probiotic microorganisms: *in vitro*, *in vivo*, genetic and omics approaches. *Front Microbiol* **6**, ID 58.
36. Koskenniemi K, Laakso K, Koponen J, Kankainen M, Greco D Auvinen P, Savijoki K, Nyman TA, et al (2011) Proteomics and transcriptomics characterization of bile stress response in probiotic *Lactobacillus rhamnosus* GG. *Mol Cell Proteomics* **10**, M110.002741.
37. Zhang X, Zhao Y, Hu Y, Liu P, Zhao L (2011) Gut Microbiota-targeted, whole-body systems biology for understanding traditional Chinese medicine. *World Sci Techol* **13**, 202–212.
38. Avonts L, De Vuyst L (2001) Antimicrobial potential of probiotic lactic acid bacteria. *Meded Rijksuniv Gent Fak Landbouwkd Toegep Biol Wet* **66**, 543–550.
39. Chang CJ, Lin CS, Lu CC, Martel J, Ko YF, Ojcius DM, Tseng SF, Wu TR. et al (2015) *Ganoderma lucidum* reduces obesity in mice by modulating the composition of the gut microbiota. *Nat Commun* **8**, ID 16130.
40. Xu J, Chen HB, Li SL (2017) Understanding the molecular mechanisms of the interplay between herbal medicines and gut microbiota. *Med Res Rev* **37**, 1140–1185.

Appendix A. Supplementary data

Table S1 Putative antimicrobial peptides in strain EU01.

AOI	Start	End	Class	Core sequence
01	1191203	1211290	Streptide	VLKRNIITVSYSKGVPNMSKELEKVLESSSMAKGDGWKVMAKGDGWE
02	911888	934657	BlpD	MATQTIENFNTLDLETLASVEGGLSCDEGMLAVGGLGAVGGPWGAVG GVLVGAALYCF
03	1597751	1617751	Sactipeptides	MYQFSLKKFSDSKSQVIKNVIDFLNNNEISLSKTNTKIVEFSTKIPLKVIQI EVTNKCNLRCMHCYLPDYSKELDRKKISSIVYEAKQLGVMDVDFTGGE PLLLQGLSEIIEEVLKEGMCTTIFTNAVYIPEDFKILIQRYDGIRLKVSLDG WNETIHDSIRGRGTFKRTIKNIEYFRSLGVPVTVNVVLNNKNISGVKYFL ELFDRLDVKYAFDRFLPFERNNRLSISDEEFNNAILCIPNIQANCNNISES TFESFYCGAGNSYVFINSSGDVGFCPTLSSTKFCGGNINEKTLNDIWINS KFFNHIRNVRCKYYNECPANYVCQGGCRSRAQFFGGSIGSPDIQECKLA YNLTGIKPKSMSL
04	619313	639313	Sactipeptides	MEELITPSEKRIINRKKGEIYDYISYSNAFVPYQGWKIHISANLIDYQSILD NVYHVCSIFQTPFKYINKISELFRILSKHVSQLEIGKFITIYPKNKETFLLL LEELYDKIPKYTGVQILTDRSYKDSEIIFYRYGVMNARLINNERPKLKFN GTFYEDITEPYYTCPPFVEDIIFNKVVDDYNIESLFHDRYQMESIIHKSGA GNVYIAIDTINEEKVIIKEARKKVYITEKILAIDLLLNEKCILKKLKGKVDI PNYIECFTIEGNLYLVEEFIDGQRLDILKPEYNLLIKRNSSELGRYNKKVK KIISNLFLSLYKIHQEGIILEDISSSNILLTNDDRVFFIDLETAYNKNDGIIV ETTNECYPKNISQKNEQRDIVKMWYCIIDLLTNSTSLLKYDNTGVSTLN LFYKMSLENNLPKSLRKKFINDFSIVDFKNTFIIKFIEMGLNIEKIVRMQQ DLTETILSHNTFEIYGKTILESIDNYKHISNMDLKFSSDPSFSSLYDNCNK SIDDLIGIAILDNNFELFLNCNLDELLHNMSYYQKYYLLRLFNDTKICDR VYFIKVLNSIIKNDIKCIDGVKYIKSNEYFSPYLITGNSGLIIELIKFSKNNN TMKFDEWIRSLSEGISYTYAKGTSLYYGLAGLGLANAWLYYYFKETSF LKTSIKICEHIFDFSIKQNTKTILIDPMSEEIDYTYSKGMLGQLYFINELLN IIKE
05	249973	292864	NRP-like peptide	MTILKTFSDTVKQYPSKVAVMYSGGEFTFQEVDVMSNFIAKQLLLNSD EETVPFYIEKNKYVLPVVLGIMKSGKIPLPITNSLEVKISLERISEVVFDVL ISDRDVKLENHSVTLLLLPKKLESYSEYQEVATTKENEIAHIICTSGTTG VPKKVFLTDDNIDWLVKEFYKIVKFTSESKFLFTTPYTFDVSLTEILAPV YTGGTLVCYDGGIQNIIRLGETIEKKKITHLSLSPSFAETIIDISGPEVFQN LRALCLAGETFPSSLANRLRGLIQQGCRVFNLYGPSETTIYATYYELKDR KYNTVPIGKPLPGVQLKIASQKENSKMAELLIGGNGVTEGYRLQPELNK AKFKLIGSNRYYVTGDYVYYQGDNLVFSSRIDSQVQVNGIRIELDEVKS IVDKLKSVKSSRVVFYKKKLVVFYEADLNIKEDIIRGLPSYLNPTVVKVE SYYLNQNRKLDVPKMLEIYYYKKQSQQGDDVRKNILDVLSKFERVDIT DLDSLELVRFYLEIEDIFDIEIKENDFYRLKSVDSIVDYIRNKSFFQERSTE PNDSFTKEHDLVNLEYNLTKMNYRYLKNIITPSPTQKRLYKNNQNRVIG FNLALEEVTYLELNKLHHIIKYLSYKIDIFRLVVEKEQTRFSIGIVNEGDY SPNIIVLNNLPTELELQGILDNIEVIPIPIIVVGTRDKKVRFYFPYHSIDASS LNKLGDTVYQLYEKKIVIDEVPSSSLVAFSQFKREVLQNDVSGDVLARL PKIKPAIEFEKLNDEVQCFQVSLPEDIKGDDVYLFTIYAISQCILSDYNLS AISGGLSLDFRDYEQFDAYDLIGDIHKKIPFQVNRTETFEEFKNSHFKILE IYRTGIDYYEIAMLGNDMSAKEVQERLNNLSLSINFIGEAFRLKDTINNII DVDFDKNFINVFVHERFAYAVIKSELLSNSVYDLMHKDSKFELKVIDKK RLENEETNR

Table S2 The upregulated genes of strain EU01 in response to AEEL (q-value < 0.005).

Gene ID	$\log_2$(fold change)	p-value	q-value	Description
STH8232_RS10220	0.38709	0	0	RNase P RNA component class B
STH8232_RS10370	0.32117	0	0	transfer-messenger RNA
STH8232_RS01325	0.00044	0	0	molecular chaperone GroEL
STH8232_RS02470	1.31790	3.54E–53	5.74E–51	competence protein CoiA
STH8232_RS03790	0.75704	6.04E–51	8.70E–49	PspC domain-containing protein
STH8232_RS02650	0.02358	3.32E–26	3.31E–24	elongation factor Tu
STH8232_RS03610	0.63606	3.40E–22	2.59E–20	catabolite control protein A
STH8232_RS09860	0.56438	3.09E–18	1.82E–16	CsbD family protein
STH8232_RS06760	0.04000	1.18E–14	5.46E–13	peptide-methionine (R)-S-oxide reductase
STH8232_RS06840	0.40506	9.24E–14	3.86E–12	hypothetical protein
STH8232_RS10955	0.59087	7.20E–12	2.59E–10	6S RNA
STH8232_RS04020	0.73130	2.95E–09	8.70E–08	hypothetical protein
STH8232_RS00510	0.92980	9.01E–09	2.59E–07	PolC-type DNA polymerase III
STH8232_RS02255	0.61957	4.14E–08	1.05E–06	DeoR/GlpR transcriptional regulator
STH8232_RS04050	0.84746	1.14E–07	2.79E–06	DUF3165 domain-containing protein
STH8232_RS06440	0.46306	3.03E–07	7.15E–06	phosphocarrier protein HPr
STH8232_RS03205	0.85117	3.79E–07	8.78E–06	VIT family protein
STH8232_RS04410	0.74300	4.05E–07	9.22E–06	deoxyribose-phosphate aldolase
STH8232_RS01320	0.08942	1.10E–06	2.41E–05	co-chaperone GroES
STH8232_RS00385	0.92164	1.81E–06	3.85E–05	transcriptional regulator Spx
STH8232_RS00875	0.00168	4.13E–06	7.99E–05	HrcA family transcriptional regulator
STH8232_RS02955	1.16460	4.51E–06	8.48E–05	glucan-binding protein
STH8232_RS05450	0.54489	1.42E–05	2.35E–04	hypothetical protein
STH8232_RS05855	0.63751	2.63E–05	4.05E–04	UDP-glucose 4-epimerase GalE
STH8232_RS07135	0.71118	6.07E–05	8.74E–04	primosomal protein N'
STH8232_RS02935	2.49180	2.33E–03	1.28E–03	CHAP domain-containing protein
STH8232_RS04435	0.97745	9.16E–05	1.28E–03	ABC transporter permease
STH8232_RS02685	1.08340	2.60E–03	1.39E–03	ammonium transporter
STH8232_RS05210	0.86359	1.22E–04	1.64E–03	transcriptional regulator Spx
STH8232_RS02970	2.39670	3.24E–03	1.65E–03	hypothetical protein
STH8232_RS07715	1.01300	3.93E–03	1.87E–03	DNA internalization-related competence protein ComEC/Rec2
STH8232_RS09935	2.78520	4.51E–03	2.04E–03	membrane protein
STH8232_RS04540	3.69210	4.57E–03	2.05E–03	cold-shock protein
STH8232_RS01130	0.61879	2.48E–04	3.05E–03	amino acid ABC transporter ATP-binding protein
STH8232_RS04780	0.33591	3.12E–04	3.71E–03	glutamine-hydrolyzing GMP synthase
STH8232_RS06725	3.65150	6.81E–04	4.00E–03	ABC transporter permease
STH8232_RS05480	6.03790	4.04E–04	4.54E–03	VanZ family protein

Table S3 The downregulated genes of strain EU01 in response to AEEL (q-value < 0.005).

Gene ID	$\log_2$(fold change)	p-value	q-value	Description
STH8232_RS02455	−1.26410	0	0	methionine–tRNA ligase
STH8232_RS08020	−0.97538	0	0	ATP-dependent Clp protease ATP-binding subunit
STH8232_RS00885	−0.80040	0	0	molecular chaperone DnaK
STH8232_RS09550	−1.32970	3.21E–93	5.94E–91	50S ribosomal protein L5
STH8232_RS03470	−0.20195	1.18E–45	1.53E–43	ATP-dependent Clp protease ATP-binding subunit
STH8232_RS07005	−0.96509	2.15E–42	2.54E–40	UDP-glucose 4-epimerase GalE
STH8232_RS06035	−0.77968	5.40E–40	5.83E–38	pyruvate kinase
STH8232_RS08845	−0.66908	4.73E–25	4.38E–23	elongation factor G
STH8232_RS00880	−0.48359	8.62E–25	7.45E–23	nucleotide exchange factor GrpE
STH8232_RS03230	−0.46928	4.20E–23	3.40E–21	pyridine nucleotide-disulfide oxidoreductase
STH8232_RS08705	−0.31225	3.29E–21	2.37E–19	DNA polymerase I
STH8232_RS08280	−1.20730	9.42E–21	6.42E–19	Xaa-Pro dipeptidyl-peptidase
STH8232_RS04010	−0.43950	2.44E–20	1.58E–18	superoxide dismutase
STH8232_RS08805	−0.88511	7.96E–20	4.91E–18	phosphoglycerate kinase
STH8232_RS08225	−0.25212	9.71E–18	5.47E–16	formate C-acetyltransferase
STH8232_RS06040	−0.57180	1.61E–16	8.70E–15	ATP-dependent 6-phosphofructokinase
STH8232_RS02635	−0.72620	2.82E–16	1.41E–14	ATP synthase subunit beta
STH8232_RS08405	−0.44488	2.79E–16	1.41E–14	ATP-dependent helicase
STH8232_RS03605	−0.56937	8.68E–16	4.17E–14	aminopeptidase P family protein
STH8232_RS08580	−0.11820	1.40E–14	6.24E–13	PTS beta-glucoside transporter subunit IIBCA
STH8232_RS04045	−0.49747	2.17E–14	9.37E–13	translational GTPase TypA
STH8232_RS09595	−0.86854	1.27E–13	5.16E–12	50S ribosomal protein L2
STH8232_RS09240	−1.15440	4.49E–13	1.71E–11	DNA-directed RNA polymerase subunit beta'
STH8232_RS07210	−0.41548	4.39E–13	1.71E–11	peptide ABC transporter substrate-binding protein
STH8232_RS02625	−0.69791	1.09E–12	4.02E–11	ATP synthase subunit alpha
STH8232_RS06425	−0.47908	8.48E–12	2.97E–10	NADP-dependent glyceraldehyde-3-phosphate dehydrogenase
STH8232_RS06435	−0.30819	1.67E–11	5.69E–10	phosphoenolpyruvate–protein phosphotransferase
STH8232_RS00550	−0.90055	5.45E–11	1.81E–09	30S ribosomal protein S2
STH8232_RS04025	−0.00680	7.34E–11	2.38E–09	DNA starvation/stationary phase protection protein
STH8232_RS01740	−1.01010	8.07E–11	2.55E–09	O-sialoglycoprotein endopeptidase
STH8232_RS09605	−0.86764	1.58E–10	4.86E–09	50S ribosomal protein L4
STH8232_RS07010	−0.50489	3.22E–10	9.72E–09	UDP-glucose–hexose-1-phosphate uridylyltransferase
STH8232_RS02490	−1.30880	9.59E–09	2.70E–07	alanine-tRNA ligase
STH8232_RS06080	−0.73319	1.19E–08	3.27E–07	2%2C3-bisphosphoglycerate-dependent phosphoglycerate mutase
STH8232_RS09510	−0.76572	1.40E–08	3.77E–07	preprotein translocase subunit SecY
STH8232_RS01880	−0.84351	2.48E–08	6.56E–07	PTS mannose/fructose/sorbose transporter subunit IIC
STH8232_RS01275	−0.94539	2.93E–08	7.60E–07	glucose-6-phosphate isomerase
STH8232_RS02630	−0.65766	5.59E–08	1.39E–06	ATP synthase subunit gamma
STH8232_RS00890	−0.18015	1.77E–07	4.25E–06	molecular chaperone DnaJ
STH8232_RS03820	−1.25910	1.10E–06	2.41E–05	U32 family peptidase
STH8232_RS09845	−0.28220	1.35E–06	2.91E–05	alkaline shock response membrane anchor protein AmaP
STH8232_RS06365	−0.20647	2.70E–06	5.65E–05	phosphoglucosamine mutase
STH8232_RS00540	−0.41675	2.99E–06	6.15E–05	alkyl hydroperoxide reductase subunit F
STH8232_RS09010	−0.78473	3.49E–06	7.07E–05	50S ribosomal protein L11
STH8232_RS09005	−0.65404	4.02E–06	7.91E–05	50S ribosomal protein L1

Table S3 Continued ...

Gene ID	$\log_2$(fold change)	*p*-value	*q*-value	Description
STH8232_RS00250	−0.42905	4.03E–06	7.91E–05	amidophosphoribosyltransferase
STH8232_RS09610	−0.75873	4.42E–06	8.42E–05	50S ribosomal protein L3
STH8232_RS09485	−1.10140	5.02E–06	9.30E–05	DNA-directed RNA polymerase subunit alpha
STH8232_RS08850	−1.14260	5.93E–06	1.08E–04	30S ribosomal protein S7
STH8232_RS08770	−0.62648	7.32E–06	1.32E–04	ribonuclease J
STH8232_RS06565	−0.96571	9.66E–06	1.72E–04	phenylalanine–tRNA ligase subunit beta
STH8232_RS00245	−0.10666	1.03E–05	1.80E–04	phosphoribosylformylglycinamidine synthase
STH8232_RS06510	−1.03100	1.27E–05	2.17E–04	L-lactate dehydrogenase
STH8232_RS02610	−0.82089	1.27E–05	2.17E–04	F0F1 ATP synthase subunit A
STH8232_RS02190	−0.87891	1.31E–05	2.20E–04	enoyl-[acyl-carrier-protein] reductase FabK
STH8232_RS08855	−1.10110	1.60E–05	2.61E–04	30S ribosomal protein S12
STH8232_RS05445	−0.26500	1.61E–05	2.61E–04	AarF/ABC1/UbiB kinase family protein
STH8232_RS09855	−0.29121	1.87E–05	2.99E–04	Asp23/Gls24 family envelope stress response protein
STH8232_RS09540	−0.96826	2.02E–05	3.19E–04	30S ribosomal protein S8
STH8232_RS00555	−0.88083	2.61E–05	4.05E–04	elongation factor Ts
STH8232_RS08075	−0.93642	2.77E–05	4.22E–04	Asp-tRNA(Asn)/Glu-tRNA(Gln) amidotransferase GatCAB subunit B
STH8232_RS02205	−0.62071	3.82E–05	5.76E–04	beta-ketoacyl-[acyl-carrier-protein] synthase II
STH8232_RS09245	−0.63743	4.56E–05	6.80E–04	DNA-directed RNA polymerase subunit beta
STH8232_RS05110	−1.15130	4.81E–05	7.09E–04	orotate phosphoribosyltransferase
STH8232_RS05955	−1.05040	5.28E–05	7.69E–04	50S ribosomal protein L19
STH8232_RS09525	−1.24170	6.82E–05	9.72E–04	30S ribosomal protein S5
STH8232_RS02740	−0.55443	8.26E–05	1.16E–03	glycine–tRNA ligase subunit beta
STH8232_RS01865	−0.31982	9.57E–05	1.32E–03	serine–tRNA ligase
STH8232_RS02370	−0.86563	9.81E–05	1.34E–03	NADP-specific glutamate dehydrogenase
STH8232_RS04285	−0.52396	1.14E–04	1.55E–03	phospho-sugar mutase
STH8232_RS07870	−0.66061	1.32E–04	1.75E–03	copper-translocating P-type ATPase
STH8232_RS09615	−0.91222	1.37E–04	1.79E–03	30S ribosomal protein S10
STH8232_RS05380	−0.87082	1.64E–04	2.13E–03	dihydrolipoyl dehydrogenase
STH8232_RS09640	−0.90080	1.95E–04	2.50E–03	adenylosuccinate synthetase
STH8232_RS01750	−1.05420	2.00E–04	2.54E–03	methionine import ATP-binding protein MetN
STH8232_RS03185	−0.97637	2.24E–04	2.82E–03	rhodanese domain-containing protein
STH8232_RS09515	−0.98780	2.29E–04	2.86E–03	50S ribosomal protein L15
STH8232_RS09535	−0.87333	2.49E–04	3.05E–03	50S ribosomal protein L6
STH8232_RS09450	−1.06930	2.55E–04	3.09E–03	fructose-1%2C6-bisphosphate aldolase%2C class II
STH8232_RS00545	−1.35230	3.10E–04	3.71E–03	peroxiredoxin
STH8232_RS08330	−0.57793	3.21E–04	3.78E–03	ComC/BlpC family peptide pheromone /bacteriocin
STH8232_RS03780	−0.59115	3.67E–04	4.28E–03	RNA-binding transcriptional accessory protein
STH8232_RS09560	−0.97789	3.73E–04	4.31E–03	50S ribosomal protein L14
STH8232_RS05385	−0.91066	3.82E–04	4.38E–03	2-oxo acid dehydrogenase subunit E2
STH8232_RS03845	−0.60126	4.07E–04	4.54E–03	divalent metal cation transporter
STH8232_RS01875	−0.50642	4.02E–04	4.54E–03	PTS mannose transporter subunit IID
STH8232_RS00320	−0.40204	4.11E–04	4.55E–03	arginine-tRNA ligase
STH8232_RS02655	−0.34657	4.41E–04	4.85E–03	triose-phosphate isomerase
STH8232_RS00645	−0.69783	4.56E–04	4.96E–03	50S ribosomal protein L13

Table S4 The most enriched KEGG pathway terms of DEGs.

Term	DEGs no.	*p*-value
Metabolic pathways	88	0.532918711
Biosynthesis of secondary metabolites	37	0.839601595
Biosynthesis of antibiotics	33	0.572968972
Ribosome	30	0.025261063
Microbial metabolism in diverse environments	24	0.296376022
Purine metabolism	21	0.085374458
Carbon metabolism	20	0.066816616
Glycolysis/Gluconeogenesis	17	0.019335806
Aminoacyl-tRNA biosynthesis	14	0.988741062
Biosynthesis of amino acids	14	0.997898614
Amino sugar and nucleotide sugar metabolism	13	0.052493342
Pyruvate metabolism	11	0.058347869
Pyrimidine metabolism	10	0.780024205
ABC transporters	10	0.990325462
RNA degradation	8	0.022448112
Fructose and mannose metabolism	8	0.043435009
Galactose metabolism	8	0.057598565
Starch and sucrose metabolism	8	0.115819707
Quorum sensing	8	0.981739514
Oxidative phosphorylation	7	0.035388494
Amino sugar and nucleotide sugar metabolism	13	0.052493342
Pyruvate metabolism	11	0.058347869
Pyrimidine metabolism	10	0.780024205
ABC transporters	10	0.990325462
RNA degradation	8	0.022448112
Fructose and mannose metabolism	8	0.043435009
Galactose metabolism	8	0.057598565
Starch and sucrose metabolism	8	0.115819707
Quorum sensing	8	0.981739514
Oxidative phosphorylation	7	0.035388494
Phosphotransferase system (PTS)	5	0.238513951
Cysteine and methionine metabolism	5	0.739265896
Two-component system	5	0.794586466
RNA polymerase	4	0.101936507
Citrate cycle (TCA cycle)	4	0.188251274
Glycine, serine and threonine metabolism	4	0.833804875
Peptidoglycan biosynthesis	4	0.892238933
Cationic antimicrobial peptide (CAMP) resistance	3	0.358597816
Selenocompound metabolism	3	0.422477769
Nucleotide excision repair	3	0.484022624
Butanoate metabolism	3	0.596450224
Protein export	3	0.732412525
Streptomycin biosynthesis	2	0.599600572
Glycerophospholipid metabolism	2	0.659851261
Glycerolipid metabolism	2	0.659851261
Base excision repair	2	0.712600926
Bacterial secretion system	2	0.831130167
Arginine biosynthesis	2	0.859566408
Valine, leucine and isoleucine biosynthesis	2	0.883560108
2-Oxocarboxylic acid metabolism	2	0.975983192
Vancomycin resistance	1	0.811768107
Nicotinate and nicotinamide metabolism	1	0.851786513
C5-Branched dibasic acid metabolism	1	0.851786513
Terpenoid backbone biosynthesis	1	0.883309756
Glyoxylate and dicarboxylate metabolism	1	0.883309756
One carbon pool by folate	1	0.943090019
Lysine biosynthesis	1	0.955213815
Pantothenate and CoA biosynthesis	1	0.978186603

Supplementary data S1

Strain screening and culture, and detection of effect of AEEL on growth of EU01 are available upon request to authors.

Effect of AEEL on the growth of EU 01 – 5 mg/ml AEEL was found to be optimum for culturing EU01 (Fig. S1a) and optimal period for promoting growth was 24 h (Fig. S1b).

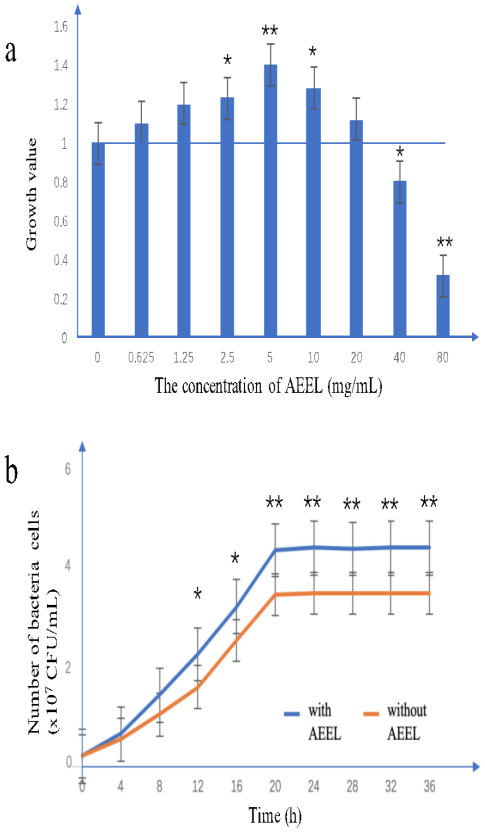

Fig. S1 Effect of AEEL on the growth of EU01. (a) The growth value of EU01 under different concentration of AEEL; (b) the growth curves of EU01 with/without AEEL.